

Ginsenoside panaxatriol reverses TNBC paclitaxel resistance by inhibiting the IRAK1/NF- κ B and ERK pathways

Panpan Wang^{Equal first author, 1, 2}, Dan Song^{Equal first author, 1}, Danhong Wan³, Lingyu Li³, Wenhui Mei³, Xiaoyun Li³, Li Han², Xiaofeng Zhu², Li Yang¹, Yu Cai^{Corresp., 1}, Ronghua Zhang^{Corresp. 1}

¹ College of Pharmacy, Jinan university, Guangzhou, China

² First Affiliated Hospital of Jinan University, Guangzhou, China

³ College of Traditional Chinese Medicine, Jinan university, Guangzhou, China

Corresponding Authors: Yu Cai, Ronghua Zhang

Email address: tcaiyu@jnu.edu.cn, tzh@jnu.edu.cn

Background. Paclitaxel (PTX) resistance is a major obstacle in the treatment of triple-negative breast cancer (TNBC). Previously, we have reported that interleukin-1 receptor-associated kinase 1 (IRAK1) and its downstream pathways are associated with PTX resistance in TNBC cells. In this study, we sought to investigate the combination treatment of ginsenoside panaxatriol (GPT), one of the main active components in Panax ginseng, with PTX on viability and apoptosis of TNBC PTX resistant cells, and explore the role of IRAK1 mediated signaling pathways in the therapeutic effects. **Methods.** CellTiter-Glo and colony formation assays were used to assess cell viability. Flow cytometry was used to analyze subG1 and apoptosis. Western blot was used to detect expressions of proteins involved in apoptosis and the IRAK1/NF- κ B and ERK pathways. The mRNA expression of inflammatory cytokines, S100A7/8/9, and cancer stem cell (CSC) -related genes were examined by qPCR. Stem cells were identified by tumor sphere assay. Cell invasion ability was examined by transwell assay. **Results.** We show that GPT inhibits MDA-MB-231 PTX resistant (MB231-PR) cell viability in a dose dependent manner. When combined with PTX, GPT synergistically causes more cell death, induces subG1 accumulation and cell apoptosis. Besides, up-regulation of BAX/BCL-2 ratio, and down-regulation of MCL-1 are also observed. Moreover, this combination inhibit IRAK1, NF- κ B and ERK1/2 activation, and lead to down-regulation of inflammatory cytokines (IL6, IL8, CXCL1, CCL2), S100A7/9, and CSC-related genes (OCT4, SOX2, NANOG, ALDH1, CD44) expression. In addition, the combination treatment suppresses MB231-PR cell invasion ability, and impairs tumor sphere growth both in MB231-PR and SUM159 PTX resistant (SUM159-PR) cells. **Conclusion.** Our study demonstrates that GPT can resensitize TNBC PTX resistant cells to PTX by inhibiting the IRAK1/NF- κ B and ERK pathways and reducing stem cell characteristics.

1 Ginsenoside panaxatriol reverses TNBC paclitaxel 2 resistance by inhibiting the IRAK1/NF- κ B and ERK 3 pathways

4 Panpan Wang ^{1,2#}, Dan Song ^{1#}, Danhong Wan ³, Lingyu Li ³, Wenhui Mei ³, Xiaoyun Li ³, Li
5 Han ², Xiaofeng Zhu ², Li Yang ¹, Yu Cai ^{1*}, Ronghua Zhang ^{1*}

6 ¹: College of Pharmacy, Jinan University, Guangzhou, Guangdong, 510630, PR China

7 ²: First Affiliated Hospital of Jinan University, Guangzhou, Guangdong, 510630, PR China

8 ³: College of Traditional Chinese Medicine, Jinan University, Guangzhou, Guangdong, 510630,
9 PR China

10 *: Correspondence:

11 Ronghua Zhang¹; Yu Cai²

12 No.601, West Huangpu Avenue, Tianhe District, Guangzhou, Guangdong, 510630, PR China.

13 Email address: ¹: tzh@jnu.edu.cn; ²: tcay@jnu.edu.cn

14 #: Co-first author

15 Abstract

16 **Background.** Paclitaxel (PTX) resistance is a major obstacle in the treatment of triple-
17 negative breast cancer (TNBC). Previously, we have reported that interleukin-1 receptor-
18 associated kinase 1 (IRAK1) and its downstream pathways are associated with PTX resistance
19 in TNBC cells. In this study, we sought to investigate the combination treatment of ginsenoside
20 panaxatriol (GPT), one of the main active components in Panax ginseng, with PTX on viability
21 and apoptosis of TNBC PTX resistant cells, and explore the role of IRAK1 mediated signaling
22 pathways in the therapeutic effects.

23 **Methods.** CellTiter-Glo and colony formation assays were used to assess cell viability. Flow
24 cytometry was used to analyze subG1 and apoptosis. Western blot was used to detect
25 expressions of proteins involved in apoptosis and the IRAK1/NF- κ B and ERK pathways. The
26 mRNA expression of inflammatory cytokines, S100A7/8/9, and cancer stem cell (CSC) -related

27 genes were examined by qPCR. Stem cells were identified by tumor sphere assay. Cell invasion
28 ability was examined by transwell assay.

29 **Results.** We show that GPT inhibits MDA-MB-231 PTX resistant (MB231-PR) cell viability
30 in a dose dependent manner. When combined with PTX, GPT synergistically causes more cell
31 death, induces subG1 accumulation and cell apoptosis. Besides, up-regulation of BAX/BCL-2
32 ratio, and down-regulation of MCL-1 are also observed. Moreover, this combination inhibit
33 IRAK1, NF- κ B and ERK1/2 activation, and lead to down-regulation of inflammatory cytokines
34 (IL6, IL8, CXCL1, CCL2), S100A7/9, and CSC-related genes (OCT4, SOX2, NANOG,
35 ALDH1, CD44) expression. In addition, the combination treatment suppresses MB231-PR cell
36 invasion ability, and impairs tumor sphere growth both in MB231-PR and SUM159 PTX
37 resistant (SUM159-PR) cells.

38 **Conclusion.** Our study demonstrates that GPT can resensitize TNBC PTX resistant cells to
39 PTX by inhibiting the IRAK1/NF- κ B and ERK pathways and reducing stem cell characteristics.

40 Introduction

41 TNBC is a highly invasive subtype of breast cancer with poor prognosis (Foulkes et al. 2010).
42 Because of the lack of hormone receptors and human epidermal growth factor receptor 2 (HER2)
43 amplification, TNBC does not respond to hormone or anti-HER2 treatment, and mainly relies on
44 traditional chemotherapy (Denkert et al. 2017). PTX-based chemotherapy regimens are the most
45 widely used first-line therapeutic strategies for clinically treatment of TNBC. Although effective
46 in the initial treatment, a subset of patients eventually develops resistance, and leads to disease
47 progression (Mustacchi & De Laurentiis 2015; Schettini et al. 2016). Hence, it is highly
48 necessary to find a solution for PTX resistance in TNBC.

49 The nuclear factor kappa B (NF- κ B) signaling pathway plays an important role in cancer
50 initiation, progression, and resistance, thus making it a good target for cancer treatment
51 (Chaturvedi et al. 2011; Hoesel & Schmid 2013; Taniguchi & Karin 2018). However, despite
52 numerous attempts to develop molecular drugs that specifically target NF- κ B, few clinical
53 advancements have been made (Baud & Karin 2009). Previously, by using gain and loss of
54 function methods, we reported that activation of interleukin-1 receptor-associated kinase 1
55 (IRAK1), an upstream kinase of the NF- κ B signaling pathway, is associated with PTX resistance

56 in TNBC cells (Wee et al. 2015). Importantly, together with S100A7, S100A8 and S100A9
57 (S100A7/8/9), IRAK1 form a druggable circuitry which drives the malignancy of TNBC cells
58 (Goh et al. 2017). These observations prompted us to search for potential candidate drugs that
59 can target IRAK1 and its downstream signaling pathways.

60 Ginseng and its active ingredient ginsenosides, such as ginsenosides Rg3 (GRg3), have been
61 widely used in China to treat cancers in the clinic. Ginsenosides are a class of steroid glycosides
62 and triterpene saponins. Over the last decade, more than 100 different types have been isolated
63 and identified. Researchers have found that GRg3 can facilitate the penetration of PTX through
64 the Caco-2 monolayer from the apical side to the basal side, and enhance the oral bioavailability
65 of PTX *in vivo* (Yang et al. 2012). Furthermore, GRg3 can inhibit P-glycoprotein expression and
66 increase the accumulation of drugs such as vincristine in multidrug resistant cells, but not in
67 sensitive cells (Kim et al. 2003). Importantly, it has been reported that some ginsenosides can
68 inhibit the activation of IRAK1 and its downstream pathways (Joh et al. 2011; Nag et al. 2012;
69 Shaukat et al. 2019). In this study, we investigated the *in vitro* anti-viability of GPT in TNBC
70 PTX resistant cells, and found that GPT can target IRAK1/NF- κ B and ERK pathways to
71 overcome resistance.

72 **Materials & Methods**

73 **Chemicals and reagents**

74 GPT was obtained from Must Bio-Technology (Chengdu, China). PTX was purchased from
75 Sigma-Aldrich (St. Louis, MO, USA). Dulbecco's Modified Eagle Medium (DMEM) (11995-
76 040), F-12 nutrient mixture (Ham) and fetal bovine serum (FBS) were bought from Life
77 Technologies (Grand Island, NY, USA). MammoCul medium (human) and supplements were
78 purchased from STEMCELL Technologies (Vancouver, Canada). CellTiter-Glo luminescent cell
79 viability assay kits were purchased from Promega Corporation (Madison, WI, USA). iScript
80 gDNA Clear cDNA Synthesis Kits and iTaq Universal SYBR Green Supermix Kits were
81 purchased from Bio-Rad Laboratories (Hercules, CA USA). p-IRAK1 S376, IRAK1, p-P65
82 S536, P65, p-ERK1/2, ERK1/2, BAX, BCL-2 and MCL-1 antibodies were supplied by Cell
83 Signaling Technology (Danvers, MA, USA). Beta-actin antibody was purchased from Sigma
84 Aldrich (St. Louis, MO, USA).

85 Cell culture and viability assay

86 MB231 cells and SUM159 cells were obtained from ATCC. MB231-PR cells and SUM159-PR
87 were established as previously described (Wee et al. 2015). Briefly, cells were treated with
88 increasing concentrations of PTX for over a period of 3 months. Then, MB231-PR cells were
89 cultured in DMEM supplemented with 75 nM PTX, penicillin/streptomycin, and 10% FBS at 37
90 °C with 5% CO₂. SUM159-PR cells were maintained in F-12 supplemented with 300nM
91 paclitaxel, 5% FBS, 10 mM HEPES, 10 µg/ml hydrocortisone, 5 µg/ml insulin and 1%
92 penicillin/streptomycin. For cell viability assay, 1000 cells/well in 90 µl medium were seeded
93 into Costar 96-well white plates. The next day, different concentrations of drugs in 10 µl medium
94 were added and incubated for the indicated times. Then, cells were lysed with 50 µl CellTiter-
95 Glo reagent and the chemiluminescent signals were detected with a PerkinElmer VICTOR X4
96 plate reader.

97 Cell cycle and apoptosis assay

98 Cell cycle and apoptosis analysis was performed by DNA content quantification to quantify the
99 subG1 population, which is a reflective of the extent of cell death. Briefly, floating and adherent
100 cells were harvested together after 48 h and 72 h treatment respectively. Then, cells were fixed
101 by 70% ethanol at 4 °C overnight. After washing with phosphate buffered saline (PBS), cells
102 were resuspended in 100µl of 100 µg/ml RNase A. 5 min later, 400µl of 50 µg/ml propidium
103 iodide were added, and cells were incubated for 30 min in dark area. Finally, the stained cells
104 were analyzed by FACScalibur and quantified using CellQuest software.

105 Colony formation assay

106 1000 cells/well were seeded into 12-well plates. The next day, drugs were added and incubated
107 for 12 days. Medium was changed every 3 days. Then, cells were washed with PBS and fixed
108 with methanol for 10 min. Finally, cells were then stained with 0.1% crystal violet at room
109 temperature for 10 min and photographed.

110 Tumor sphere formation assay

111 3000 cells/well in 180 μ l medium were seeded into Corning 96-well spheroid microplates in
112 complete MammoCul medium. The next day, drugs in 20 μ l medium were added and incubated
113 for 12 days. Pictures were taken on day 6 and day 12. Finally, on day 12, cells were lysed with
114 100 μ l CellTiter-Glo reagent and the chemiluminescent signal was detected with a PerkinElmer
115 VICTOR X4 plate reader.

116 Transwell invasion assay

117 10000 cells in 100 μ l serum-free DMEM containing DMSO, PTX, GPT, or combination were
118 added into Corning Transwell polycarbonate membrane inserts coated with Matrigel (300
119 μ g/mL). And medium containing 10% FBS was added to the bottom chamber. After 24 h
120 incubation, the cells that remained on the above surface of the insert membrane were scraped off
121 with a cotton swab. The cells that passed through Matrigel to the bottom of the insert were fixed
122 with paraformaldehyde and stained with 0.1% crystal violet in methanol. The inserts were
123 photographed, and the cells were counted.

124 Quantitative-PCR (qPCR) assay

125 RNA extraction and purification were performed according to the instructions from Zymo
126 Research (R2052). 750 ng RNA was used to synthesize cDNA. And qPCR was performed using
127 the Applied Biosystems 7500 Fast Real-Time PCR system. All primers are listed in table 1. For
128 quantification of mRNA levels, 18S was used as the internal control, and the expression of target
129 genes were analyzed using the $2^{-\Delta\Delta CT}$ method.

130 Western blot assay

131 Western blot was performed using whole-cell extracts in protein lysis buffer with freshly added
132 protease inhibitor cocktail. Proteins were separated on 8%–10% SDS polyacrylamide gel
133 electrophoresis gels and transferred to polyvinylidene difluoride membranes. The membrane was
134 blocked with 5% non-fat dry milk in tris-buffered saline (TBS) containing 0.1% Tween 20
135 (TBST). The membrane was then incubated with primary antibody (1:1000 dilution) in 5%
136 bovine serum albumin overnight. After washed 3 times with TBST, the membrane was incubated

137 with secondary antibody (1:2000 dilution) in 5% non-fat dry milk at room temperature for 1 h.
138 Then, SuperSignal West Femto Maximum Sensitivity Substrate was added, and images were
139 taken using the ChemiDoc MP System.

140 **Statistical analysis**

141 Data are shown as mean \pm SD. The t test was used to determine whether there are any
142 statistically significant differences between two groups. $P < 0.05$ was considered statistically
143 significant.

144 **Results**

145 **GPT promotes cytotoxicity of PTX in MB231-PR cells**

146 To explore whether GPT can promote cytotoxicity of PTX in TNBC resistant cells, MB231-PR
147 was constructed and used as cell model. Firstly, we conducted CellTiter-Glo assay to observe
148 different concentration of GPT on cell viability. As shown in Fig. 1A, GPT treatment
149 significantly decreased cell viability of MB231-PR cells in a dose dependent manner, with the
150 half maximal inhibitory concentration (IC₅₀) 21.39 μ M. Secondly, we combined GPT with PTX
151 to check whether they have synergistic effects. Results showed that the combination caused
152 dramatic cell death in a dose and time dependent manner, comparing to either single use group
153 (Fig. 1B). Interestingly, the synergistic effects didn't apply to MB231 parental (MB231-PT)
154 cells, although MB231-PT cells were sensitive to PTX (Fig. S1) and showed more sensitive to
155 GPT when treated with the same concentration (Fig. 1C). Notable, the clinical using drug GRg3
156 didn't cause significant cell death in single or combination treatment group (Fig. S2). In addition,
157 colony formation assay confirmed the synergistic cytotoxicity effects of the combination on
158 MB231-PR cells (Fig. 1D, Fig. S3).

159 Since chemotherapy resistance appears partly due to aberrant changes of signaling pathways that
160 endowed cells with the abilities to escape apoptosis, restoring apoptosis is a very important
161 therapeutic strategy for antitumor therapy (Baig et al. 2016; Plati et al. 2008). Therefore, next,
162 we used flow cytometry to measure subG1 changes after the combination treatment, which is
163 marker of apoptosis. Not surprisingly, GPT combined with PTX significantly increased subG1

164 cell accumulation both after 48 h and 72 h (Fig. 1E, *Fig. S4*). Taken together, these results
165 suggested GPT as a very effective molecular to reverse PTX resistance in TNBC cells.

166 **The combination treatment activates mitochondria mediated apoptosis**

167 The alteration of pro-apoptotic proteins and anti-apoptotic proteins play important roles in the
168 determination of cancer cells apoptosis, and are associated with chemoresistance (Campbell &
169 Tait 2018; Warren et al. 2019). Thus, we observed the protein expression of BAX and BCL-2
170 after treatment, two key mediators of apoptotic response to chemotherapy. As shown in Fig 2A-
171 B, GPT combined with PTX significantly increased BAX and decreased BCL-2 expression in a
172 dose and time dependent manner.

173 Besides BAX and BCL-2, MCL-1 was recently reported to be associated with poor prognosis in
174 TNBC patients and can be used as a therapeutic target (Campbell et al. 2018). Notably, we have
175 shown that IRAK1 inhibitor can decrease MCL-1 expression in MB321-PR cells to induce cell
176 apoptosis (Wee et al. 2015). Therefore, we also evaluated the protein expression of MCL-1 after
177 treatment. As shown in Fig. 2A-B, the combination treatment also resulted in down-regulation of
178 MCL-1 expression. These results together suggested that the combination treatment activated
179 mitochondria mediated apoptosis to reverse PTX resistance.

180 **The combination treatment inhibits IRAK1/NF- κ B and ERK pathways**

181 To further clarify the signaling pathways that involved in GPT effects, gene expression profiling
182 was conducted in MB231-PR cells treated with DMSO, PTX, GPT, and combination,
183 respectively. Results showed that NOD-like receptor signaling pathways played an important
184 part in GPT activity in MB231-PR cells (data not shown). Interestingly, through loss and gain of
185 function study, we have previously reported that activation of IRAK1, a key kinase of NOD-like
186 receptor signaling pathway, is associated with PTX resistance in TNBC cells (Wee et al. 2015)
187 Moreover, target IRAK1 using pharmacologic inhibitor can induce MB231-PR cells apoptosis,
188 when combined with PTX (Wee et al. 2015) Thus, consideration was given to IRAK1 and its
189 downstream signaling pathways. Results showed that the combination treatment can significantly
190 inhibit the phosphorylation of IRAK1, P65, ERK1/2, and increase the expression of I κ B-alpha in
191 a dose and time dependent manner (Fig. 2A-B).

192 To additionally characterize the functional effects of IRAK1 mediated pathways, we investigated
193 the mRNA expression of NF- κ B target genes by qPCR, including interleukin 6 (IL6), IL8,
194 chemokine (C-X-C motif) ligand 1 (CXCL1), and chemokine (C-C motif) ligand 2 (CCL2). The
195 above cytokines were shown to be distinctly expressed among different group in our gene
196 expression profiling experiment, and were reported to be critical for the anchorage independent
197 growth of TNBC cells (Hartman et al. 2013). As shown in Fig. 2C-F, (*Table S1, Table S3*),
198 compared to DMSO, PTX significantly promoted the expression of IL6, IL8, CXCL1 and CCL2.
199 However, this induction can be significantly attenuated when combined with GPT.
200 Except these target cytokines, we previously published that IRAK1 and S100A7/8/9 form a
201 feedback loop to drive the malignancy of TNBC cells (Goh et al. 2017). Here, we also showed
202 that the combination treatment significantly decreased S100A7 and S100A9 mRNA expression
203 (Fig. 2G-H, *Table S1, Table S3*), although S100A8 mRNA expression level was too low to
204 detect. These results together suggested that the combination treatment overcome PTX resistance
205 by inhibiting IRAK1 mediated NF- κ B and ERK pathways.

206 **The combination treatment inhibits CSC-related genes expression and impairs tumor** 207 **sphere growth and invasion ability**

208 Accompanied with killing cancer cell, PTX treatment has been reported to induce CSC
209 enrichment, another key mechanism suggested to be responsible for chemoresistance and cancer
210 metastasis (Bousquet et al. 2017; Zhang et al. 2019). And drug that can target cancer stemness
211 are proposed as new strategies for clinical cancer treatment (Saygin et al. 2019; Sun et al. 2019).
212 In order to testify the effect of combination therapy on characteristics of CSC, firstly, qPCR was
213 used to check the expression of a group of CSC-related genes. As shown in Fig. 3A-E, (*Table*
214 *S2, Table S4, Table S5*), compared to PTX, the combination treatment significantly lead to
215 down-regulation of octamer-binding transcription factor 4 (OCT4), sex determining region Y-
216 box 2 (SOX2), NANOG, aldehyde dehydrogenase 1 (ALDH1), and CD44 gene expression.
217 Secondly, transwell invasion and tumor sphere assay were conducted to assess CSC properties.
218 As shown in Fig. 3F and 3G-J, the combination treatment significantly suppressed MB231-PR
219 cell invasion ability, and impaired tumor sphere growth both in MB231-PR and SUM159-PR
220 cells.

221 Discussion

222 Treatment of TNBC has been challenging, due to lack of target therapy options and constantly
223 acquired resistance. Therefore, a combinatorial therapy has been always preferred to achieve a
224 synergistic effects. Plant derived compounds, such as saponins, flavonoids and alkaloids, have
225 been tested and proved to be effective in killing cancer cells and restoring resistant cells to
226 chemotherapy (Aung et al. 2017). Of which, ginsenosides have been researched in different
227 cancers. Results showed that GRg3 can enhance the anti-cancer ability of chemo drugs by
228 modulating the oral bioavailability (Yang et al. 2012), inhibiting P-glycoprotein expression (Kim
229 et al. 2003), inhibiting cell autophagy (Wang et al. 2019), and down regulating epidermal growth
230 factor receptor (EGFR)/ phosphatidylinositol-3-kinase (PI3K)/ Akt signaling pathway (Jiang et
231 al. 2017). In this study, we investigated the combination treatment of GPT and PTX on viability
232 and apoptosis of TNBC PTX resistant cells, and clarified the signaling pathways underlies. Our
233 data showed that the combination can synergistically inhibit MB231-PR cell viability, induce
234 subG1 accumulation and trigger the mitochondrial mediated apoptosis. Our data further
235 suggested that the combination can inhibit IRAK1/NF- κ B and ERK signaling pathways, resulted
236 in down-regulation of inflammatory factors and S100A7/9 expression, which are the main
237 cytokines in tumor microenvironment contributed to CSC phenotype and function. In addition,
238 we showed that combination can inhibit CSC-related genes expression and impair invasion
239 ability and tumor sphere growth.

240 It is suggested that the BCL-2 family are key mediators of anti-cancer therapeutics, and
241 abnormal expression of apoptotic proteins contributed to chemoresistance (Hata et al. 2015). In
242 addition to other members, decreased BAX/BCL-2 ratio and elevated MCL-1 expression were
243 reported to be closely related with PTX resistance in breast cancer (Lee et al. 2017; Sharifi et al.
244 2014). Drugs which can inhibit the activity of these proteins are believed to improve the efficacy
245 of chemotherapeutic agents. Interestingly, our data showed that GPT augments the effects of
246 PTX by up-regulating BAX/BCL-2 ratio and down-regulating MCL-1 expression.

247 The results in this study are consistent with our previous published papers, showing that
248 pharmacologic inhibition of IRAK1 phosphorylation and downstream signaling pathways
249 activation can overcome TNBC PTX resistance. Notably, other group recently reported that the
250 expression of IRAK1 was positively correlated with tumor size following neoadjuvant
251 chemotherapy (NCT) (Yang et al. 2019). Breast cancer patients, with higher expression of

252 IRAK1 both before and after NCT, had a shorter survival period (Yang et al. 2019). These
253 results together highlight the role of IRAK1 in chemoresistance and clinical application of
254 IRAK1 inhibitors. I κ B-alpha is a downstream kinase of IRAK1. It has been reported that I κ B-
255 alpha plays an important role in NF- κ B cytosolic-nuclear translocation. I κ B-alpha enters the
256 nucleus to bind NF- κ B dimers and translocate them to the cytosol(Christian et al. 2016).
257 Researchers also showed that I κ B-alpha was the key mediator responsible for PTX induced NF-
258 κ B nuclear translocation, DNA binding and transcriptional activity (Huang et al. 2000).
259 Consistently, decreased I κ B-alpha and increased NF- κ B transcriptional activity after PTX
260 treatment can also be seen in our experiment. However, the combination treatment increased
261 I κ B-alpha expression and decreased NF- κ B transcriptional activity.
262 Another our major finding is that inhibition of IRAK1/NF- κ B and ERK pathways by GPT
263 reduced stem cell characteristics. CSCs have been reported as one of the determining reasons for
264 chemoresistance and subsequent cancer relapse. And one of the mechanisms that CSCs are
265 acquired is taking advantage of PTX treatment induced inflammation cytokines and S100 protein
266 family in tumor microenvironment.
267 In our experiment, decreased expression of inflammation cytokines (IL-6, IL-8, CXCL1 and
268 CCL2) can be noticed in the combination group. The above cytokines are reported to be NF- κ B
269 transcriptional targets, and their expression are induced following NF- κ B activation after chemo
270 treatment (Jia et al. 2017). In turn, these factors activate inflammation related signaling pathways
271 such as NF- κ B and signal transducer and activator of transcription 3 (STAT3) (Wang et al. 2018;
272 Wong et al. 2015; Yue et al. 2006), which further promote cell survival through regulating
273 apoptosis proteins and promote the formation of CSC through regulating CSC related genes
274 (Rhyasen et al. 2013). Importantly, in accordance to IL-8 inhibitor, anti-IL6 antibody, anti-
275 CXCL1 antibody, or anti-CCL2 antibody, here we showed that target IRAK1 mediated pathways
276 by ginsenoside PPT can effectively down-regulate these cytokines and disrupt this process (Dey
277 et al. 2019; Heo et al. 2016; Miyake et al. 2019; Teng et al. 2017).
278 Besides, we also identified that S100A7/9 were down-regulated after combination treatment.
279 S100A7/9 are members of the S100 protein family, which are closely related to tumorigenesis
280 and progression (Cancemi et al. 2018; Chen et al. 2014). In addition, S100A7/8/9 can be
281 regulated by NF- κ B and STAT3, which in turn can activate NF- κ B and ERK (Hermani et al.
282 2006; Liu et al. 2013; Nemeth et al. 2009). S100A8/9 and CXCL1/2, or S100A7/8/9 and IRAK1,

283 form a feedback loop to cause cancer chemoresistance and drive breast cancer tumor sphere
284 growth (Acharyya et al. 2012; Goh et al. 2017). Collectively, our data suggested that GPT can
285 disrupt this feedback loop to inhibit CSC characteristics.
286 As to molecular phenotype in breast cancer, CSCs display CD44+/CD24- phenotype and high
287 ALDH1 activity. In parallel, other characters include overexpression of transcription factors
288 OCT4, SOX2 and NANOG, which are associated with high-grade stage and poor clinical
289 outcome in TNBC. In this part, we demonstrated that GPT combined with PTX can inhibit CSCs
290 related gene expression, impair invasion ability and tumor sphere growth.

291 **Conclusions**

292 Our study demonstrates that GPT can resensitize TNBC PTX resistant cells to PTX treatment by
293 inhibiting the IRAK1/NF- κ B and ERK pathways, reducing stem cell characteristics, thus provide
294 it as a novel molecular for clinic use.

295 **Acknowledgements**

296 We thank all the reviewers for their helpful comments.

297 **References**

- 298 Acharyya S, Oskarsson T, Vanharanta S, Malladi S, Kim J, Morris PG, Manova-Todorova K,
299 Leversha M, Hogg N, Seshan VE, Norton L, Brogi E, and Massague J. 2012. A CXCL1
300 paracrine network links cancer chemoresistance and metastasis. *Cell* 150:165-178.
301 10.1016/j.cell.2012.04.042
- 302 Aung TN, Qu Z, Kortschak RD, and Adelson DL. 2017. Understanding the Effectiveness of
303 Natural Compound Mixtures in Cancer through Their Molecular Mode of Action. *Int J Mol*
304 *Sci* 18. 10.3390/ijms18030656
- 305 Baig S, Seevasant I, Mohamad J, Mukheem A, Huri HZ, and Kamarul T. 2016. Potential of
306 apoptotic pathway-targeted cancer therapeutic research: Where do we stand? *Cell*
307 *Death Dis* 7:e2058. 10.1038/cddis.2015.275
- 308 Baud V, and Karin M. 2009. Is NF-kappaB a good target for cancer therapy? Hopes and pitfalls.
309 *Nat Rev Drug Discov* 8:33-40. 10.1038/nrd2781
- 310 Bousquet G, El Bouchtaoui M, Sophie T, Leboeuf C, de Bazelaire C, Ratajczak P, Giacchetti S,
311 de Roquancourt A, Bertheau P, Verneuil L, Feugeas JP, Espie M, and Janin A. 2017.
312 Targeting autophagic cancer stem-cells to reverse chemoresistance in human triple
313 negative breast cancer. *Oncotarget* 8:35205-35221. 10.18632/oncotarget.16925
- 314 Campbell KJ, Dhayade S, Ferrari N, Sims AH, Johnson E, Mason SM, Dickson A, Ryan KM,
315 Kalna G, Edwards J, Tait SWG, and Blyth K. 2018. MCL-1 is a prognostic indicator and
316 drug target in breast cancer. *Cell Death Dis* 9:19. 10.1038/s41419-017-0035-2
- 317 Campbell KJ, and Tait SWG. 2018. Targeting BCL-2 regulated apoptosis in cancer. *Open Biol*
318 8. 10.1098/rsob.180002

- 319 Cancemi P, Buttacavoli M, Di Cara G, Albanese NN, Bivona S, Pucci-Minafra I, and Feo S.
320 2018. A multiomics analysis of S100 protein family in breast cancer. *Oncotarget*
321 9:29064-29081. 10.18632/oncotarget.25561
- 322 Chaturvedi MM, Sung B, Yadav VR, Kannappan R, and Aggarwal BB. 2011. NF-kappaB
323 addiction and its role in cancer: 'one size does not fit all'. *Oncogene* 30:1615-1630.
324 10.1038/onc.2010.566
- 325 Chen H, Xu C, Jin Q, and Liu Z. 2014. S100 protein family in human cancer. *Am J Cancer Res*
326 4:89-115.
- 327 Christian F, Smith EL, and Carmody RJ. 2016. The Regulation of NF-kappaB Subunits by
328 Phosphorylation. *Cells* 5. 10.3390/cells5010012
- 329 Denkert C, Liedtke C, Tutt A, and von Minckwitz G. 2017. Molecular alterations in triple-negative
330 breast cancer-the road to new treatment strategies. *Lancet* 389:2430-2442.
331 10.1016/s0140-6736(16)32454-0
- 332 Dey P, Rathod M, and De A. 2019. Targeting stem cells in the realm of drug-resistant breast
333 cancer. *Breast Cancer (Dove Med Press)* 11:115-135. 10.2147/bctt.S189224
- 334 Foulkes WD, Smith IE, and Reis-Filho JS. 2010. Triple-negative breast cancer. *N Engl J Med*
335 363:1938-1948. 10.1056/NEJMra1001389
- 336 Goh JY, Feng M, Wang W, Oguz G, Yatim S, Lee PL, Bao Y, Lim TH, Wang P, Tam WL,
337 Kodahl AR, Lyng MB, Sarma S, Lin SY, Lezhava A, Yap YS, Lim AST, Hoon DSB, Ditzel
338 HJ, Lee SC, Tan EY, and Yu Q. 2017. Chromosome 1q21.3 amplification is a trackable
339 biomarker and actionable target for breast cancer recurrence. *Nat Med* 23:1319-1330.
340 10.1038/nm.4405
- 341 Hartman ZC, Poage GM, den Hollander P, Tsimelzon A, Hill J, Panupinthu N, Zhang Y,
342 Mazumdar A, Hilsenbeck SG, Mills GB, and Brown PH. 2013. Growth of triple-negative
343 breast cancer cells relies upon coordinate autocrine expression of the proinflammatory
344 cytokines IL-6 and IL-8. *Cancer Res* 73:3470-3480. 10.1158/0008-5472.Can-12-4524-t
- 345 Hata AN, Engelman JA, and Faber AC. 2015. The BCL2 Family: Key Mediators of the Apoptotic
346 Response to Targeted Anticancer Therapeutics. *Cancer Discov* 5:475-487.
347 10.1158/2159-8290.Cd-15-0011
- 348 Heo TH, Wahler J, and Suh N. 2016. Potential therapeutic implications of IL-6/IL-6R/gp130-
349 targeting agents in breast cancer. *Oncotarget* 7:15460-15473.
350 10.18632/oncotarget.7102
- 351 Hermani A, De Servi B, Medunjanin S, Tessier PA, and Mayer D. 2006. S100A8 and S100A9
352 activate MAP kinase and NF-kappaB signaling pathways and trigger translocation of
353 RAGE in human prostate cancer cells. *Exp Cell Res* 312:184-197.
354 10.1016/j.yexcr.2005.10.013
- 355 Hoesel B, and Schmid JA. 2013. The complexity of NF-kappaB signaling in inflammation and
356 cancer. *Mol Cancer* 12:86. 10.1186/1476-4598-12-86
- 357 Huang Y, Johnson KR, Norris JS, and Fan W. 2000. Nuclear factor-kappaB/IkappaB signaling
358 pathway may contribute to the mediation of paclitaxel-induced apoptosis in solid tumor
359 cells. *Cancer Res* 60:4426-4432.
- 360 Jia D, Li L, Andrew S, Allan D, Li X, Lee J, Ji G, Yao Z, Gadde S, Figeys D, and Wang L. 2017.
361 An autocrine inflammatory forward-feedback loop after chemotherapy withdrawal
362 facilitates the repopulation of drug-resistant breast cancer cells. *Cell Death Dis* 8:e2932.
363 10.1038/cddis.2017.319
- 364 Jiang J, Yuan Z, Sun Y, Bu Y, Li W, and Fei Z. 2017. Ginsenoside Rg3 enhances the anti-
365 proliferative activity of erlotinib in pancreatic cancer cell lines by downregulation of
366 EGFR/PI3K/Akt signaling pathway. *Biomed Pharmacother* 96:619-625.
367 10.1016/j.biopha.2017.10.043

- 368 Joh EH, Lee IA, Jung IH, and Kim DH. 2011. Ginsenoside Rb1 and its metabolite compound K
369 inhibit IRAK-1 activation--the key step of inflammation. *Biochem Pharmacol* 82:278-286.
370 10.1016/j.bcp.2011.05.003
- 371 Kim SW, Kwon HY, Chi DW, Shim JH, Park JD, Lee YH, Pyo S, and Rhee DK. 2003. Reversal
372 of P-glycoprotein-mediated multidrug resistance by ginsenoside Rg(3). *Biochem*
373 *Pharmacol* 65:75-82. 10.1016/s0006-2952(02)01446-6
- 374 Lee KM, Giltneane JM, Balko JM, Schwarz LJ, Guerrero-Zotano AL, Hutchinson KE, Nixon MJ,
375 Estrada MV, Sanchez V, Sanders ME, Lee T, Gomez H, Lluch A, Perez-Fidalgo JA, Wolf
376 MM, Andrejeva G, Rathmell JC, Fesik SW, and Arteaga CL. 2017. MYC and MCL1
377 Cooperatively Promote Chemotherapy-Resistant Breast Cancer Stem Cells via
378 Regulation of Mitochondrial Oxidative Phosphorylation. *Cell Metab* 26:633-647.e637.
379 10.1016/j.cmet.2017.09.009
- 380 Liu H, Wang L, Wang X, Cao Z, Yang Q, and Zhang K. 2013. S100A7 enhances invasion of
381 human breast cancer MDA-MB-468 cells through activation of nuclear factor-kappaB
382 signaling. *World J Surg Oncol* 11:93. 10.1186/1477-7819-11-93
- 383 Miyake M, Furuya H, Onishi S, Hokutan K, Anai S, Chan O, Shi S, Fujimoto K, Goodison S, Cai
384 W, and Rosser CJ. 2019. Monoclonal Antibody against CXCL1 (HL2401) as a Novel
385 Agent in Suppressing IL6 Expression and Tumoral Growth. *Theranostics* 9:853-867.
386 10.7150/thno.29553
- 387 Mustacchi G, and De Laurentiis M. 2015. The role of taxanes in triple-negative breast cancer:
388 literature review. *Drug Des Devel Ther* 9:4303-4318. 10.2147/dddt.S86105
- 389 Nag SA, Qin JJ, Wang W, Wang MH, Wang H, and Zhang R. 2012. Ginsenosides as Anticancer
390 Agents: In vitro and in vivo Activities, Structure-Activity Relationships, and Molecular
391 Mechanisms of Action. *Front Pharmacol* 3:25. 10.3389/fphar.2012.00025
- 392 Nemeth J, Stein I, Haag D, Riehl A, Longerich T, Horwitz E, Breuhahn K, Gebhardt C,
393 Schirmacher P, Hahn M, Ben-Neriah Y, Pikarsky E, Angel P, and Hess J. 2009. S100A8
394 and S100A9 are novel nuclear factor kappa B target genes during malignant progression
395 of murine and human liver carcinogenesis. *Hepatology* 50:1251-1262.
396 10.1002/hep.23099
- 397 Plati J, Bucur O, and Khosravi-Far R. 2008. Dysregulation of apoptotic signaling in cancer:
398 molecular mechanisms and therapeutic opportunities. *J Cell Biochem* 104:1124-1149.
399 10.1002/jcb.21707
- 400 Rhyasen GW, Bolanos L, Fang J, Jerez A, Wunderlich M, Rigolino C, Mathews L, Ferrer M,
401 Southall N, Guha R, Keller J, Thomas C, Beverly LJ, Cortelezzi A, Oliva EN, Cuzzola M,
402 Maciejewski JP, Mulloy JC, and Starczynowski DT. 2013. Targeting IRAK1 as a
403 therapeutic approach for myelodysplastic syndrome. *Cancer Cell* 24:90-104.
404 10.1016/j.ccr.2013.05.006
- 405 Saygin C, Matei D, Majeti R, Reizes O, and Lathia JD. 2019. Targeting Cancer Stemness in the
406 Clinic: From Hype to Hope. *Cell Stem Cell* 24:25-40. 10.1016/j.stem.2018.11.017
- 407 Schettini F, Giuliano M, De Placido S, and Arpino G. 2016. Nab-paclitaxel for the treatment of
408 triple-negative breast cancer: Rationale, clinical data and future perspectives. *Cancer*
409 *Treat Rev* 50:129-141. 10.1016/j.ctrv.2016.09.004
- 410 Sharifi S, Barar J, Hejazi MS, and Samadi N. 2014. Roles of the Bcl-2/Bax ratio, caspase-8 and
411 9 in resistance of breast cancer cells to paclitaxel. *Asian Pac J Cancer Prev* 15:8617-
412 8622. 10.7314/apjcp.2014.15.20.8617
- 413 Shaukat A, Guo YF, Jiang K, Zhao G, Wu H, Zhang T, Yang Y, Guo S, Yang C, Zahoor A,
414 Akhtar M, Umar T, Shaukat I, Rajput SA, Hassan M, and Deng G. 2019. Ginsenoside
415 Rb1 ameliorates Staphylococcus aureus-induced Acute Lung Injury through attenuating
416 NF-kappaB and MAPK activation. *Microb Pathog* 132:302-312.
417 10.1016/j.micpath.2019.05.003

- 418 Sun HR, Wang S, Yan SC, Zhang Y, Nelson PJ, Jia HL, Qin LX, and Dong QZ. 2019.
419 Therapeutic Strategies Targeting Cancer Stem Cells and Their Microenvironment. *Front*
420 *Oncol* 9:1104. 10.3389/fonc.2019.01104
- 421 Taniguchi K, and Karin M. 2018. NF-kappaB, inflammation, immunity and cancer: coming of
422 age. *Nat Rev Immunol* 18:309-324. 10.1038/nri.2017.142
- 423 Teng KY, Han J, Zhang X, Hsu SH, He S, Wani NA, Barajas JM, Snyder LA, Frankel WL,
424 Caligiuri MA, Jacob ST, Yu J, and Ghoshal K. 2017. Blocking the CCL2-CCR2 Axis
425 Using CCL2-Neutralizing Antibody Is an Effective Therapy for Hepatocellular Cancer in a
426 Mouse Model. *Mol Cancer Ther* 16:312-322. 10.1158/1535-7163.Mct-16-0124
- 427 Wang J, Tian L, Khan MN, Zhang L, Chen Q, Zhao Y, Yan Q, Fu L, and Liu J. 2018.
428 Ginsenoside Rg3 sensitizes hypoxic lung cancer cells to cisplatin via blocking of NF-
429 kappaB mediated epithelial-mesenchymal transition and stemness. *Cancer Lett* 415:73-
430 85. 10.1016/j.canlet.2017.11.037
- 431 Wang XJ, Zhou RJ, Zhang N, and Jing Z. 2019. 20(S)-ginsenoside Rg3 sensitizes human non-
432 small cell lung cancer cells to icotinib through inhibition of autophagy. *Eur J Pharmacol*
433 850:141-149. 10.1016/j.ejphar.2019.02.023
- 434 Warren CFA, Wong-Brown MW, and Bowden NA. 2019. BCL-2 family isoforms in apoptosis and
435 cancer. *Cell Death Dis* 10:177. 10.1038/s41419-019-1407-6
- 436 Wee ZN, Yatim SM, Kohlbauer VK, Feng M, Goh JY, Bao Y, Lee PL, Zhang S, Wang PP, Lim
437 E, Tam WL, Cai Y, Ditzel HJ, Hoon DS, Tan EY, and Yu Q. 2015. IRAK1 is a therapeutic
438 target that drives breast cancer metastasis and resistance to paclitaxel. *Nat Commun*
439 6:8746. 10.1038/ncomms9746
- 440 Wong AS, Che CM, and Leung KW. 2015. Recent advances in ginseng as cancer therapeutics:
441 a functional and mechanistic overview. *Nat Prod Rep* 32:256-272. 10.1039/c4np00080c
- 442 Yang LQ, Wang B, Gan H, Fu ST, Zhu XX, Wu ZN, Zhan DW, Gu RL, Dou GF, and Meng ZY.
443 2012. Enhanced oral bioavailability and anti-tumour effect of paclitaxel by 20(s)-
444 ginsenoside Rg3 in vivo. *Biopharm Drug Dispos* 33:425-436. 10.1002/bdd.1806
- 445 Yang M, Qin X, Qin G, and Zheng X. 2019. The role of IRAK1 in breast cancer patients treated
446 with neoadjuvant chemotherapy. *Onco Targets Ther* 12:2171-2180.
447 10.2147/ott.S185662
- 448 Yue PY, Wong DY, Wu PK, Leung PY, Mak NK, Yeung HW, Liu L, Cai Z, Jiang ZH, Fan TP,
449 and Wong RN. 2006. The angiosuppressive effects of 20(R)- ginsenoside Rg3. *Biochem*
450 *Pharmacol* 72:437-445. 10.1016/j.bcp.2006.04.034
- 451 Zhang S, Zhang H, Ghia EM, Huang J, Wu L, Zhang J, Lam S, Lei Y, He J, Cui B, Widhopf GF,
452 2nd, Yu J, Schwab R, Messer K, Jiang W, Parker BA, Carson DA, and Kipps TJ. 2019.
453 Inhibition of chemotherapy resistant breast cancer stem cells by a ROR1 specific
454 antibody. *Proc Natl Acad Sci U S A* 116:1370-1377. 10.1073/pnas.1816262116
455

Figure 1

GPT combined with paclitaxel (PTX) inhibit MB231-PR cell viability and induce cell apoptosis

(A) Single treatment of GPT on MB231-PR cell viability. Cells were treated with different concentration of GPT for 4 days. (B) Combination treatment of GPT and PTX on MB231-PR cell viability. Cells were treated with DMOS, 75 nM PTX, 10 μ M GPT, 75 nM PTX + 2.5 μ M GPT, 75 nM PTX + 5 μ M GPT, 75 nM PTX + 10 μ M GPT, respectively. (C) Combination treatment of GPT and PTX on MB231-PT cell viability. Cells were treated with DMSO, 1 nM PTX, 10 μ M GPT, and different combination, respectively. (D) Representative images of colony formation assay. MB321-PR cells were treated for 12 days with DMSO, 75 nM PTX, 10 μ M GPT and combination, respectively. (E) Flow cytometry detection of cell cycle after treatment for 48 h and 72 h. **P < 0.01, ****P < 0.0001. P-values were calculated with t test.

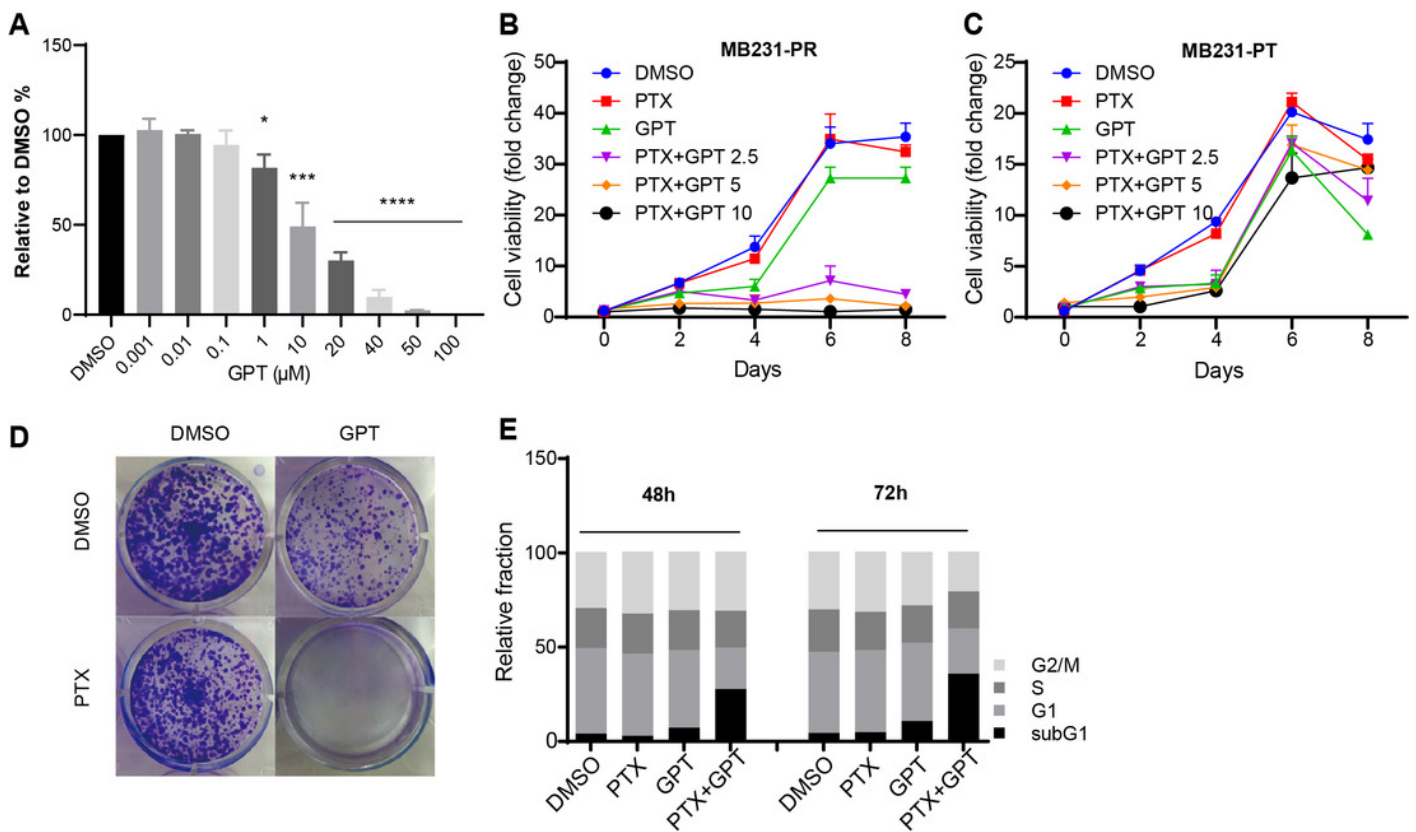


Figure 2

The combination treatment activates apoptosis pathway and inhibits IRAK1/NF- κ B, ERK pathways in MB231-PR cells

(A) Western blot analysis of proteins expression after cells treated with DMSO, 75 nM PTX, 10 μ M GPT, and different combination for 24 h. (B) Western blot analysis of proteins expression after cells treated with DMSO, 75 nM PTX, 10 μ M GPT, and combination for 24 h and 48 h, respectively. (C-H) qPCR analysis of IRAK1/NF- κ B downstream inflammatory cytokines and S100A7/9 gene expression after cells treated for 24 h and 48 h, respectively. *P < 0.05, **P < 0.01, ***P < 0.001, ****P < 0.0001. P-values were calculated with t test.

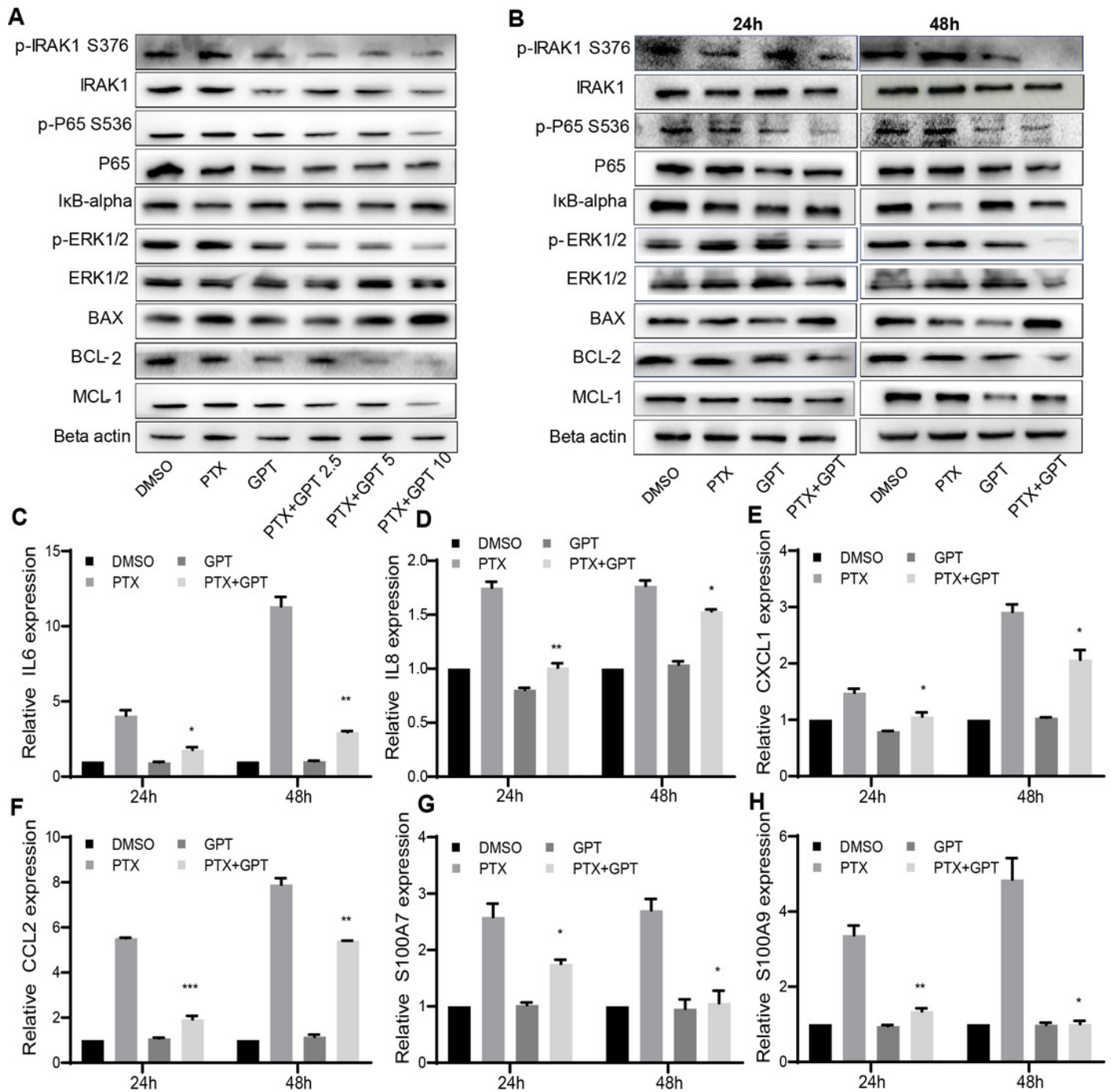


Figure 3

The combination treatment inhibits inflammatory cytokines expression, tumor sphere growth and cell invasion ability

(A-E) qPCR analysis of CSC-related genes expression after cells treated with DMSO, 75 nM PTX, 10 μ M GPT, and combination for 24 h and 48 h, respectively. (F) Transwell invasion assay of MB231-PR cells after drug treatment. Cells were seeded into Corning transwell polycarbonate membrane inserts coated with Matrigel (300 μ g/mL) and cultured for 24 h. (G-J) Representative images of tumor sphere assays. Cells were seeded into Corning 96-well spheroid microplates and cultured with MammoCul medium. Tumor sphere was observed after treated for 12 days. *P < 0.05, **P < 0.01, ***P < 0.001. P-values were calculated with t test.

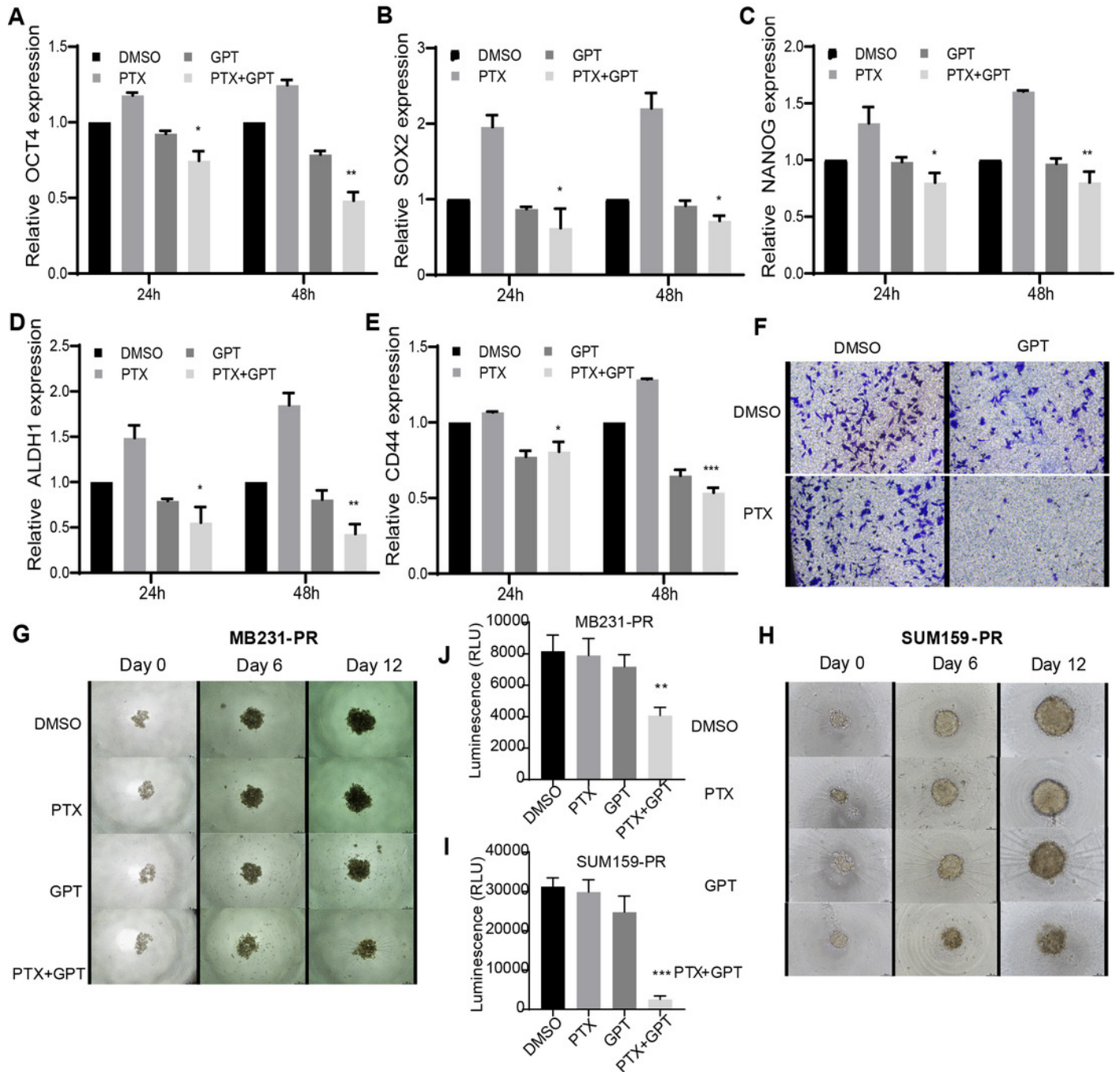


Table 1 (on next page)

qPCR primers

Table 1 qPCR primers

Gene	forward (5'-3')	reverse (5'-3')
IL6	AGTTCCTGCAGAAAAAGGCAAAG	AAAGCTGCGCAGAATGAGAT
IL8	ACCGGAAGGAACCATCTCAC	GGCAAAACTGCACCTTCACAC
CXCL1	CCAGCTCTTCCGCTCCTC	CACGGACGCTCCTGCTG
CCL2	CCCAAAGAAGCTGTGATCTTCA	TCTGGGGAAAGCTAGGGGAA
S100A7	GACAAGATTGAGAAGCCAAGCC	TGTGCCCTTTTTGTACACAGG
S100A8	TGCCGTCTACAGGGATGAC	TCTGCACCCTTTTTCTGATATAC
S100A9	TCCTCGGCTTTGACAGAGTG	TGGTCTCTATGTTGCGTTCCA
OCT4	CTGGGTTGATCCTCGGACCT	CCATCGGAGTTGCTCTCCA
SOX2	GCCGAGTGGAACTTTTTGTCG	GGCAGCGTGTACTTATCCTTCT
NANOG	TTTGTGGGCCTGAAGAAAACCT	AGGGCTGTCCTGAATAAGCAG
ALDH1	CTGCTGGCGACAATGGAGT	GTCAGCCCAACCTGCACAG
CD44	TGCCGCTTTGCAGGTGTATT	CCGATGCTCAGAGCTTTCTCC
18S	CGAACGTCTGCCCTATCAACTT	ACCCGTGGTCACCATGGTA